Construction and Building Materials 65 (2014) 367–375

Contents lists available at ScienceDirect

Construction and Building Materials

journal homepage: www.elsevier.com/locate/conbuildmat

Experimental investigation on evaporation rate for enhancing evaporative cooling effect of permeable pavement materials

Hui Li [a,*], John Harvey [a], Zhesheng Ge [b,c]

[a] University of California Pavement Research Center, Department of Civil and Environmental Engineering, University of California, Davis, CA 95616, USA
[b] School of Civil Engineering and Transportation, South China University of Technology, Guangzhou, Guangdong 510641, China
[c] State Key Laboratory of Subtropical Building Science, South China University of Technology, Wushan, Tianhe, Guangzhou, Guangdong 510640, China

HIGHLIGHTS

- A simple test method of evaporation rate was developed.
- Evaporation rate were measured for six permeable pavement materials.
- Main factors affecting evaporation rate were explored.
- Methods to enhance evaporation rate were proposed.

ARTICLE INFO

Article history:
Received 13 March 2014
Received in revised form 25 April 2014
Accepted 2 May 2014

Keywords:
Heat island
Thermal environment
Livability
Cool pavements
Permeable pavements
Evaporation cooling effect

ABSTRACT

Beyond the environmental function of stormwater management, permeable pavement is also a type of cool pavement that can help mitigate urban heat island effect through evaporative cooling. Evaporation rate is an important factor that influences the evaporative cooling effect of permeable pavements. A simple experiment method was used to initially explore the evaporation rates of different pavement materials under outdoor conditions. Experimental results of the evaporation rates were obtained for six different permeable pavement materials plus the bare water. The main factors influencing the evaporation rates were revealed. The findings imply that high water availability near the surface or large moisture exposure to the atmosphere are critical for the evaporation rate and consequent evaporative cooling effect of pavement materials. Increased air voids and permeability is one way to improve moisture exposure to the atmosphere and enhance the evaporation. Keeping the surface wet through enhanced capillary effect with finer gradations or directly sprinkling water on the surface is another way to produce a better evaporative cooling effect. An optimal design of materials with appropriately balanced pore size and capillary effect and adequate permeability is desired to maximize the evaporative cooling effect.

1. Introduction

1.1. Background

Cool pavement strategies can be used to mitigate urban heat island effects and improve outdoor thermal environments in urban areas. Improved outdoor thermal environments in urban areas could potentially help reduce the negative impacts of heat islands such as increased air conditioning (A/C) energy consumption of buildings and vehicles and impaired air quality (ground-level ozone) [1–10]. In addition, as a strategy to reduce Vehicle Miles Traveled (VMT) by creating livable and walkable communities, improving the street thermal environment is attracting increasing attention from practitioners, academics and competing industries [11–15]. Increased walking or cycling also provides an opportunity for improving human health and thus improving the quality of life [16,17].

With respect to the pavement type, the heat island might not just be a "black or white" issue (asphalt versus concrete, although it is known that albedo is a function of material microstructure and rugosity not just color), but also might be an "impervious and pervious" issue. To mitigate local heat islands and reduce the associated impacts mentioned previously, some impervious surface coverage can be substituted by pervious coverage. This is also the requirement for limiting disruption of natural hydrology according to LEED [18], which requires different options for project sites with impervious area greater or less than 50%. Permeable pavement, as

* Corresponding author. Tel.: +1 530 574 5812; fax: +1 530 752 9189.
E-mail address: hili@ucdavis.edu (H. Li).

http://dx.doi.org/10.1016/j.conbuildmat.2014.05.004
0950-0618/

a Low Impact Development (LID), can help minimize the impervious surfaces and could potentially improve the quality of life in a community and reduce other environmental impacts, such as reduced or at least slowed (where there is not full infiltration) stormwater runoff and associated water pollution, reduced stormwater management facilities, enhanced on-site infiltration for vegetation growth and recharging of underground water [1,2,19–24].

As one potential cool pavement type, permeable pavements have many environmental benefits beyond conventional impermeable pavements as mentioned above (note that asphalt, concrete and integrated concrete paver pavements can be considered for applications as permeable pavements). The main potential cooling mechanisms for permeable pavements are evaporative cooling [25,26], heat resistance [3,25,26] or reflection and evaporative cooling if using reflective permeable pavement [26,27].

Evaporation is energy transmitted away from the pavement surface by the latent heat of water vapor to achieve the phase change of water from liquid to gas. Water from moist soil or wet surface changes to vapor when heated by the solar heat or other heat sources. Water vapor then rises into the atmosphere, taking the solar energy with it and resulting in cooling effect. The evaporation term also includes evapotranspiration, a more complicated process plants use to keep cool. During evapotranspiration, water is drawn from the soil by the roots of the plant and is evaporated through stoma on the plant's leaves. Both evaporation and evapotranspiration increase when there is more moisture available, when wind speeds are greater and when the air is drier and warmer [28]. The evaporation latent heat loss q_{evap} (W/m^2) (i.e. theoretically maximum cooling effect) can be described as follows when water is completely exposed to air:

$$q_{evap} = L \cdot ER \tag{1}$$

where, ER is the evaporation rate; L is specific latent heat of water vaporization.

The evaporative cooling could reduce pavement temperature and consequent air temperature through latent heat absorbed during the phase change of water (from liquid to gas) when moisture exists in the pavement or in the underlying soil or is sprinkled on the pavement surface. Permeable pavements can provide these benefits. From the equation above, it is known that the latent heat loss (q_{evap}) from pavement is linearly and positively correlated with the evaporation rate (ER) for water exposed to air. The effect of evaporative cooling of permeable pavement highly depends on the evaporation rate of the permeable pavement materials [25,26]. Therefore, it is of great interest to explore and better understand the evaporation rate for different pavement materials used for permeable pavements.

1.2. Objective and scope of this study

The objective of this study is to measure and compare the evaporation rate of different pavement materials under outdoor conditions, and provide a better understanding and typical values of evaporation rate that are useful for the modeling and simulation of the cooling effect of evaporation from permeable pavements, and explore the first-order factors affecting the evaporation rate of permeable pavement materials.

2. Materials and methods

2.1. Description of test materials

The materials used for measurement of evaporation rate include water in six different pavement materials along with fully exposed water for comparison. These six pavement materials fall into two categories: permeable pavement surface layer materials and base layer materials or bedding layer materials. All these six types of materials are open-graded materials used in experimental pavement sections constructed at the University of California Pavement Center (UCPRC) test facilities in Davis, California.

A total of nine experimental pavement sections (A1–3, B1–3, and C1–3) were constructed for the cool pavement study at UCPRC. These nine test sections include three different pavement surfacing materials, namely integrated concrete pavers (surfacing type A), open-graded asphalt concrete (surfacing type B) and portland cement concrete (surfacing type C). For each pavement surface type, one impermeable pavement design (design 1) and two permeable pavement designs (design 2 and design 3, can also be referred to as porous or pervious depending on the material, the word permeable is used for convenience in this paper) were constructed. Six out of the nine sections are permeable pavements. Each section is 4 m by 4 m square in size (see Refs. [25–27,29] for more details).

Three permeable pavement surface layer materials were chosen for the evaporation testing in this paper, which are permeable asphalt B3 and permeable concretes C2 and C3. The permeable asphalt B2 is open graded asphalt concrete with a nominal maximum aggregate size (NMAS) of 9.5 mm and PG 64-10 asphalt binder. The main differences between permeable concrete C2 and C3 are the gradation and cement type. The C2 used a finer gradation with an NMAS of 4.75 mm and conventional gray cement, while C3 used a coarse gradation with the NMAS of 9.5 mm and a whiter cement. Due to the whiter cement with much lighter color, the C3 concrete sample has an albedo of 0.26 which is larger than that of 0.18 for the C2 concrete sample (see Table 1).

The three base layer materials or bedding layer materials include gravel S1 and S2 and sand S3. The gravel S1 was used as open-graded base aggregate reservoir layers in the six experimental permeable pavement sections mentioned above. The size of S1 is 19 mm. The gravel S2 is ASTM #8 aggregate (with NMAS of 12.5 mm, finer than S1) and was used as bedding layer materials for permeable paver sections A2 and A3. The gravel S3 is ASTM C33 sand (with NMAS of 9.5 mm, finer than S2) and was used as bedding layer material for impermeable paver section A1. In addition, a fully exposed water sample S0 was used for reference and comparison.

The gradations of these six materials are presented in Fig. 1. The C3 has the same NMAS as the B3, which is 9.5 mm. However, the C3 is more open-graded with more coarse aggregate compared to B3, as shown in Fig. 1. The gravel S1 is coarsest material followed by the S2 while the sand S3 is the finest material.

In addition to the gradation, the albedo, permeability, air void content and density of these materials were measured and listed in Table 1for reference (see Refs. [25,27,29,30] for details on measurements). The summary of each material along with material designs and other characteristics is listed in Table 1.

2.2. Experimental plan

The samples of these materials were put into 100 mm diameter × 150 mm height plastic cylinder containers (Fig. 2). The sample of permeable asphalt B3 was thin (60 mm), and the gravel S1 (19 mm NMAS) was used to fill up the cylinder (Fig. 2b) under the permeable asphalt B3, simulating the full permeable pavement structure (surface layer + reservoir layer).

Each dry sample and the cylinder container was then weighed together and recorded as m_1. The water was then added into each container slowly, ensuring it was filled up with water (Fig. 3). The permeable pavement or aggregate base will not be full of water and only partially saturated for most of time and regions. However, to simulate the permeable pavement just after the heavy rain event or extensive irrigation, the cylinders were first completely filled with water and allowed the water level to drop through evaporation. This will provide the opportunity of well monitoring the change of evaporation rate over time and better investigating the effect of water level on evaporation rate. The overflow and surface water was dried using a towel. Then the total weight of sample, container and water was measured and recorded as m_{20}. After that, the samples in containers were moved outdoors and placed under the sun for evaporation (Fig. 4). The total weight of each sample plus the container and remaining water was measured over time t and recorded as m_{2t}. The water weight left in the container at time t would be

$$m_{wt} = m_{2t} - m_1 \tag{2}$$

where m_{wt} is the mass (kg) of water left in the container at time t; m_{2t} is the total mass (kg) of a sample plus the container and remaining water at time t; m_1 is the total mass (kg) of a sample plus the container.

The weight loss (i.e. the water evaporated) over time t for each sample under outdoor conditions can be calculated as

$$\Delta m_{wt} = m_{20} - m_{2t} \tag{3}$$

where Δm_{wt} is the mass (kg) of water evaporated from the container at time t; m_{20} is the initial total mass (kg) of a sample plus the container and remaining water at time 0; m_{20} is the total mass (kg) of a sample plus the container and remaining water at time t.

The evaporation rate (ER, in kg/m^2/h or mm/h) during the time period t_1 through t_2 will be

$$ER = (m_{2t1} - m_{2t2})/[A(t_2 - t_1)] \tag{4}$$

Table 1
Characteristics of permeable pavement materials used in this paper.

Material #	Material type (NMAS)[a]	Thickness (mm)	Albedo[b]	Permeability[c] (cm/s)	Air void (%)	Density (kg/m^3)
B2	Asphalt-O (9.5 mm) + Aggregate-O (19 mm)	60 + 90	0.08	0.11	12	2270
C2	Concrete-O (4.75 mm, #4)	150	0.18	0.21	15	1980
C3	Concrete-O (9.5 mm) – white cement	150	0.26	0.29	17	2050
S1	Aggregate-O (19 mm, ~ASTM #57)	150	0.18	2.5	46	1650
S2	Aggregate-O (12.5 mm, ASTM #8)	150	0.20	1.2	25	2100
S3	Sand (9.5 mm, ASTM C33)	150	0.30	5×10^{-3}	15	2400
S0	Bare water	150	–[d]	–[d]	–[d]	1000

[a] O = Open graded.
[b] Using dual-pyranometer (see [27]).
[c] Using ASTM C1701 method (see [29]).
[d] – = Not applicable.

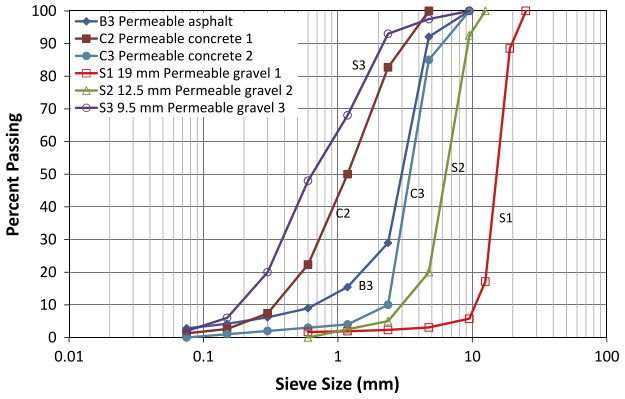

Fig. 1. Gradations of materials tested in this paper.

Fig. 3. Adding water to fill up the cylinder containers.

where ER is evaporation rate, in kg/m^2/h or mm/h; m_{2t1} is the total mass (kg) of a sample plus the container and remaining water at time t_1 (h); m_{2t2} is the total mass (kg) of a sample plus the container and remaining water at time t_2 (h); A is the sample surface area, in m^2.

The latent heat flux q_{evap} (kJ/m^2/h) lost from evaporation (i.e. cooling effect) could be calculated as

$$q_{evap} = L \cdot ER \quad (5)$$

where q_{evap} is the theoretically maximum latent heat flux lost from evaporation (i.e. cooling effect), in kJ/m^2/h; L is the specific latent heat for water vaporization, 2260 kJ/kg; ER is the evaporation rate of water, in kg/m^2/h or mm/h.

In addition, temperatures on the surfaces of the different materials were also measured using a thermometer. The weather data (including air temperature, relative humidity, solar radiation, wind speed, rain and air pressure) were also monitored using a nearby weather station. The evaporation test was conducted on clear summer days in July 2012 (July 9–25) at Davis, California. The weights and the surface temperatures for each sample were manually measured every hour. The weather data was automatically measured every half hour. The data in the first three days (July 9–11) are presented in this paper (same trends for other days).

2.3. Data analysis and presentation

The weather data, the surface temperature, the water weight left in the containers, the evaporation rate and the latent heat loss of each sample are plotted using time series plots over the experimental period (July 9–11) to examine the changes in these fundamental variables over time. In addition, the average evaporation rate over three days (July 9–11) and one day (July 10) were statistically analyzed and plotted using boxplots for each type of materials, to compare the differences in

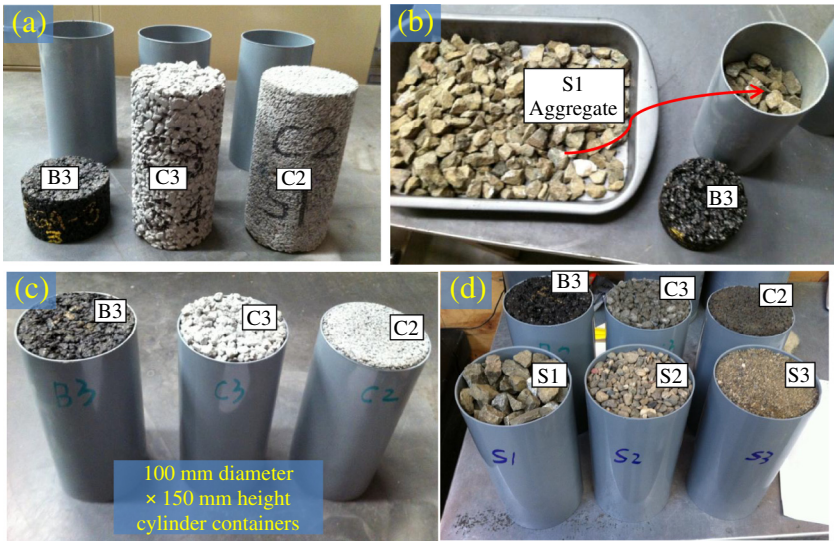

Fig. 2. Sample preparation (B3, C3 and C2 are dark due to wetting in (d)).

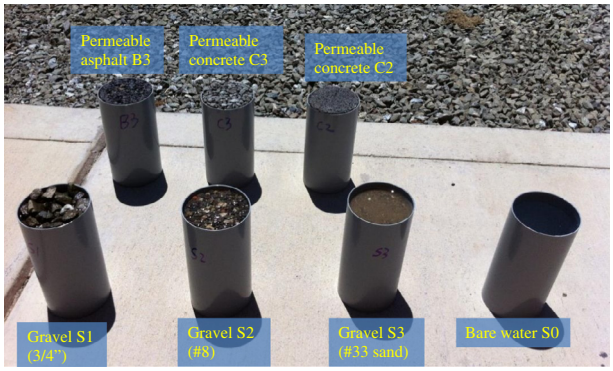

Fig. 4. Evaporation testing under outdoor conditions.

evaporation rate between materials and provide average values of evaporation rate for each materials under clear summer days. The effects of permeability and air void content and the water level depth on the evaporation rate are also examined through data plotting.

3. Results and discussion

3.1. Weather data and surface temperature change over time

The weather data during the experimental period of July 9–11, 2012 are plotted in Fig. 5. The weather was clear and sunny with high air temperatures of 36–39 °C. The peak solar radiation intensity around noon was approximately 1000 W/m^2 for all three days. The wind speed was lower than 2 m/s for most time. The low daytime relative humidity was approximately 20% while the night daytime relative humidity was approximately 80%. The weather conditions in these three days were close to each other, except the air temperature on the third day (July 11) was slightly higher than the other two days.

The surface temperatures of each sample are presented in Fig. 6. The asphalt sample has the highest surface temperature during evaporation testing due to its dark color and low albedo of 0.08 (see Table 1), which absorbs more solar energy compared to the other surfaces with higher albedos. The peak surface temperature is approximately 50 °C in the first experiment day (July 9), and reaches 60 °C on the third day (July 11). The gravel sample S3 (sand) shows the lowest surface temperature due to its higher albedo of 0.30 (see Table 1) and highest evaporation rate (see below for more details), except for the bare water S0.

3.2. Water weight change over time

The water weight change over time is presented in Fig. 7. The bare water (S0) has the most water available and the largest change rate (slope of the curve). The gravel samples S1, S2 and S3 also have relatively larger change rates. The permeable concrete samples C3 and C2 and the permeable asphalt sample B3 have relatively smaller change rates. This implies that the permeable concrete samples C3 and C2 and the permeable asphalt sample B3 have lower evaporation rates compared to the gravels (S1–S3) or the bare water (S0). The reason for their low evaporation rates might be the low air void content and low permeability of these

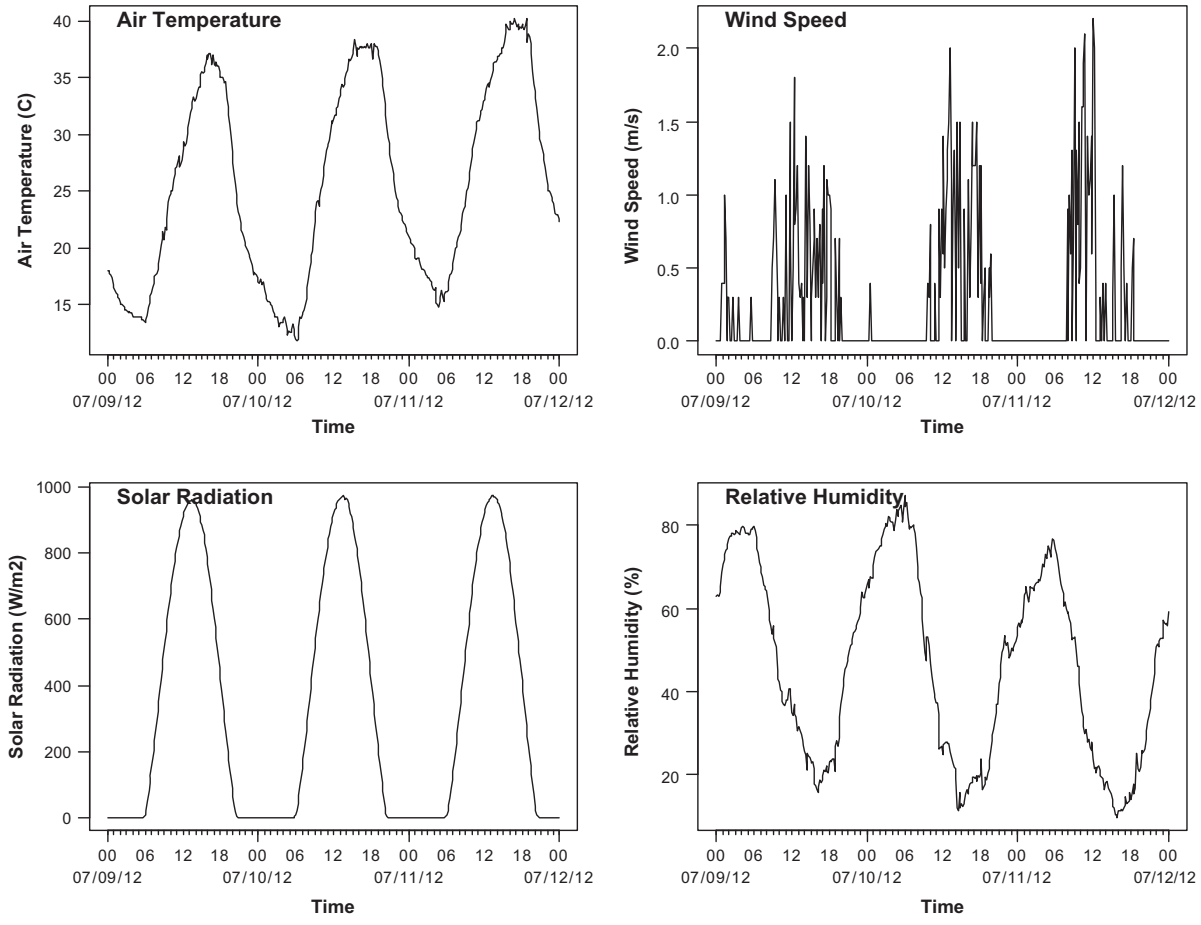

Fig. 5. Weather data during the experiment period (no rain).

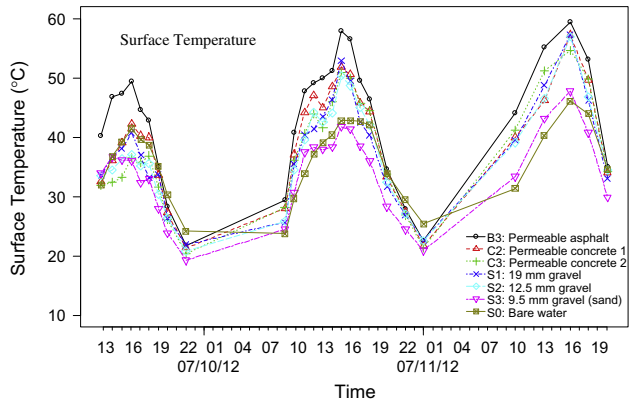

Fig. 6. Surface temperature change over time.

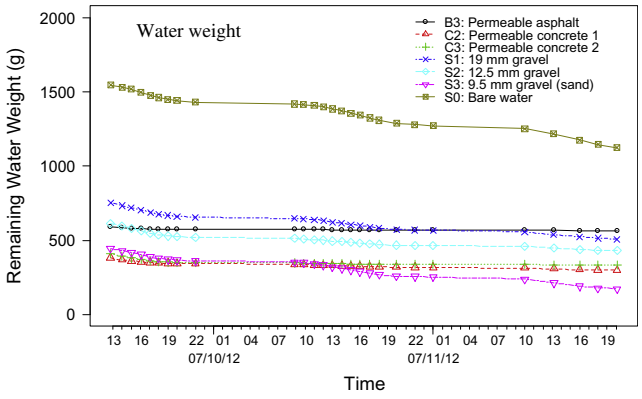

Fig. 7. Water weight change over time.

materials (see Table 1), which to some extent blocks the water evaporation from the materials. It should be noted that all samples still had more than 200 g of water available in the container even at the end of the third day (July 11).

3.3. Evaporation rate and cooling effect (latent heat flux) change over time

Fig. 8 presents the evaporation rate and latent heat loss change over time for different materials. The evaporation rates of all materials show a pattern similar to that of the air temperature, which is high in the daytime and low in the nighttime. The bare water shows the highest evaporation rate. The daily peak evaporation rate reaches 2.5 mm/h in the first day and reduces to 1.5 mm/h in the third day, although the air temperature is slightly higher in the third day (see Fig. 5). Excluding the bare water, the gravel sample S3 (sand) generally has the highest evaporation rate apparently due to its ability to move moisture to the surface for evaporation through capillary action; its peak evaporation rate drops from 1.8 mm/h in the first day to 1.0 mm/h in the third day. The surface materials of permeable concrete C2 and permeable asphalt B3 have the lowest evaporation rates, which are slightly lower than that of permeable concrete C3. Permeable concretes C3 and C2 and permeable asphalt B3 have much higher evaporation rates (0.5–1.5 mm/h) during the first experiment day when more water is available near the surfaces. Evaporation rates are lower (0.1–0.3 mm/h) in the second and third day with less moisture available near their surfaces, although there still is adequate water available in the lower part of the containers and samples.

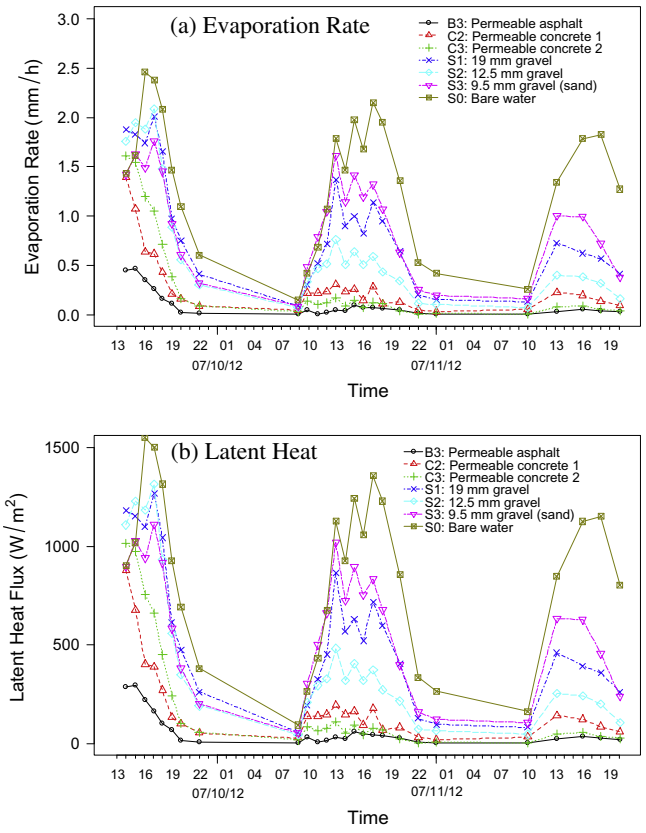

Fig. 8. Evaporation rate (a) and latent heat flux (cooling effect) and (b) change over time.

3.4. Average evaporation rates of different materials for different periods

The evaporation rates over different time frames during the experimental period (July 9–11, 2012) are calculated and plotted in Fig. 9 using boxplots for different materials, including over the three days (July 9–11), over the whole middle day (July 10), in the morning, noon, afternoon and night of the middle day (July 10). In addition, the descriptive statistics, including the number of measurement (*N*), mean, standard deviation (Std.Dev.), minimum (Min), 1st quartile (Q1), median, 3rd quartile (Q3), and maximum (Max), of the evaporation rate for two main periods (3-day and 1-day) are presented in Table 2 for reference.

Fig. 9(a) and (b) shows the evaporation rates over the three days (July 9–11) and over one day (July 10), respectively. Overall, the 3-day average evaporation rates are slightly higher than the 1-day average due to the high availability of water close to surfaces and consequently the high evaporation rates in the first day (July 9, see Fig. 7). This suggests that the availability of water close to surfaces is an important factor that influences the evaporation rate.

It is noted that the evaporation rate is high during the daytime, especially in the hot afternoon in summer (Fig. 9(d) and (e)), and low during the night time and especially in the cold early morning (Fig. 9(c) and (f)). As expected, the air temperature (also air humidity) also plays a vital role in the evaporation rate of the pavement materials. High air temperature and low humidity will help enhance the evaporation rate, which is just what is expected during hot period.

3.5. Effects of permeability and air void content on evaporation rate

In order to examine the effects of permeability and air void content on evaporation rate, the medians (highlighted in Table 2,

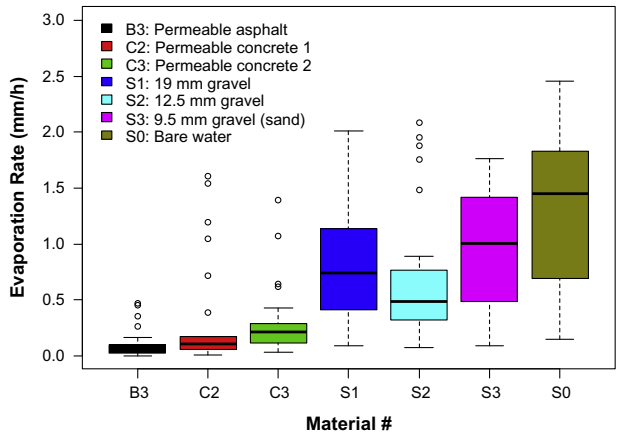

(a) 3-day Average (July 9 – July 11)

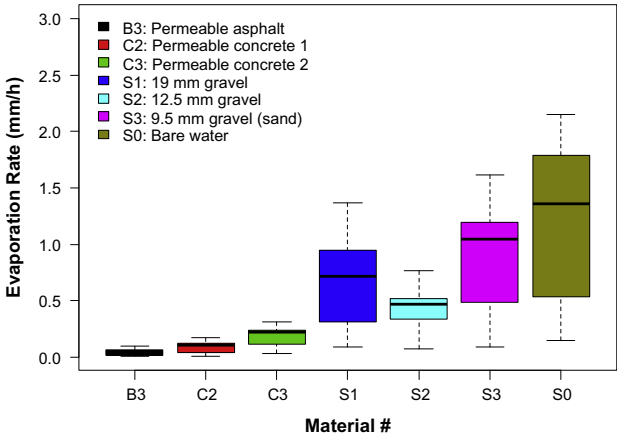

(b) 1-day Average (July 10)

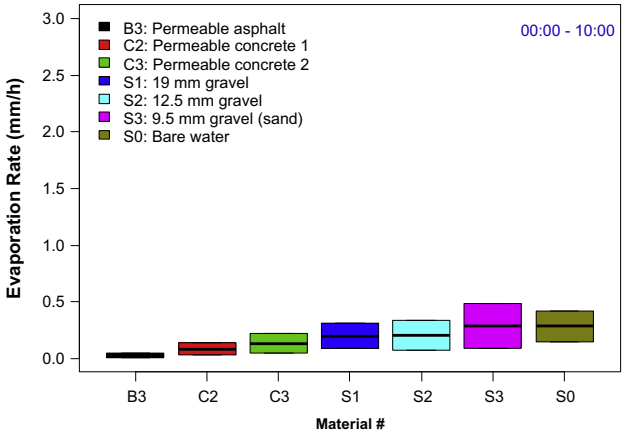

(c) Morning (00:00 – 10:00, July 10)

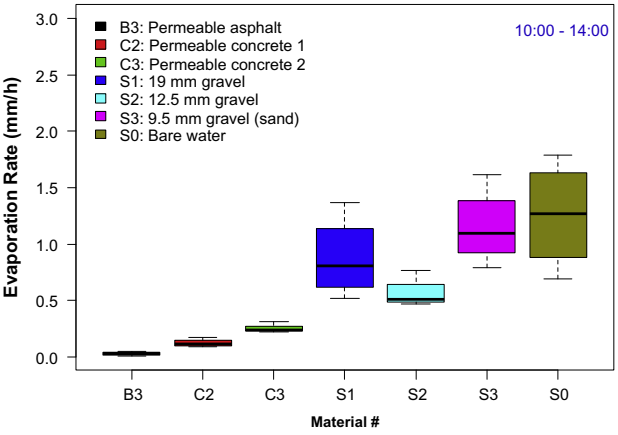

(d) Noon (10:00 – 14:00, July 10)

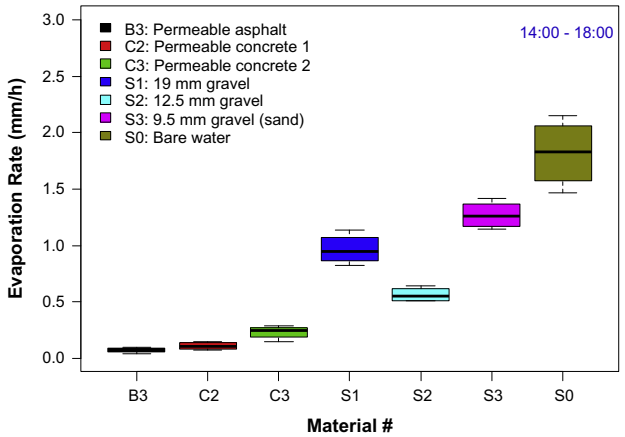

(e) Afternoon (14:00 – 18:00, July 10)

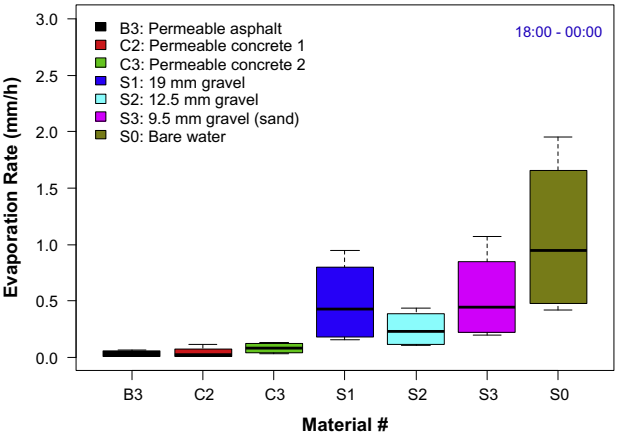

(f) Night (18:00 – 00:00, July 10)

Fig. 9. Average evaporation rates of different materials. (The center thick black horizontal line in each box of the boxplots is the median value. The colored box indicates the 1st quartile (Q1) and the 3rd quartile (Q3). The bars outside the box are the minimum and maximum values except for outliers. The circles are outliers defined as being more than 1.5 (Q3–Q1) from the Q1 or Q3.) (For interpretation of the references to colour in this figure legend, the reader is referred to the web version of this article.)

which removes the impact of outliers shown in Fig. 9(a)) of evaporation rate over the three days (July 9–11) were plotted against the permeability and air void content of different pavement materials (except the bare water), as shown in Fig. 10.

Except S3 (sand) and S0 (bare water), the evaporation rate rank is S1, S2, C3, C2 and B3. This is the same rank as the air void and permeability for these materials. The S1 (19 mm gravel) has larger air void content (46%, see Table 1) and higher permeability (0.29 cm/s, see Table 1), and largest evaporation rate (0.8 mm/h, 3-day average) compared to S2, C3, C2 and B3 (Fig. 9(a) and (b)). Among S1, S2, C3, C2 and B3, the B3 (9.5 mm) has the smallest air void content (12%) and lowest permeability (0.11 cm/s), and the smallest evaporation rate (0.1 mm/h, 3-day average). This implies that the air void and permeability are positively correlated to the evaporation rate for these permeable surface layer materials and permeable gravel materials. A small air void and low

Table 2
Descriptive statistics of the evaporation rate for different periods.

Period	Sample ID	*N*	Mean	Std.Dev.	Min	Q1	Median	Q3	Max
3-day (July 9–11)	B3	26	0.10	0.13	0.00	0.02	**0.05**	0.09	0.47
	C2	26	0.31	0.48	0.00	0.06	**0.11**	0.17	1.61
	C3	26	0.29	0.32	0.03	0.12	**0.22**	0.28	1.39
	S0	26	1.36	0.67	0.15	0.78	**1.45**	1.82	2.46
	S1	26	0.87	0.57	0.09	0.44	**0.74**	1.10	2.01
	S2	26	0.68	0.61	0.07	0.32	**0.49**	0.73	2.08
	S3	26	0.93	0.51	0.09	0.51	**1.00**	1.39	1.76
1-day (July 10)	B3	13	0.04	0.03	0.01	0.01	**0.05**	0.06	0.10
	C2	13	0.09	0.05	0.01	0.04	**0.11**	0.13	0.17
	C3	13	0.18	0.10	0.03	0.11	**0.22**	0.23	0.31
	S0	13	1.20	0.69	0.15	0.53	**1.36**	1.79	2.15
	S1	13	0.68	0.40	0.09	0.31	**0.72**	0.95	1.37
	S2	13	0.41	0.21	0.07	0.33	**0.47**	0.52	0.76
	S3	13	0.87	0.50	0.09	0.48	**1.05**	1.20	1.62

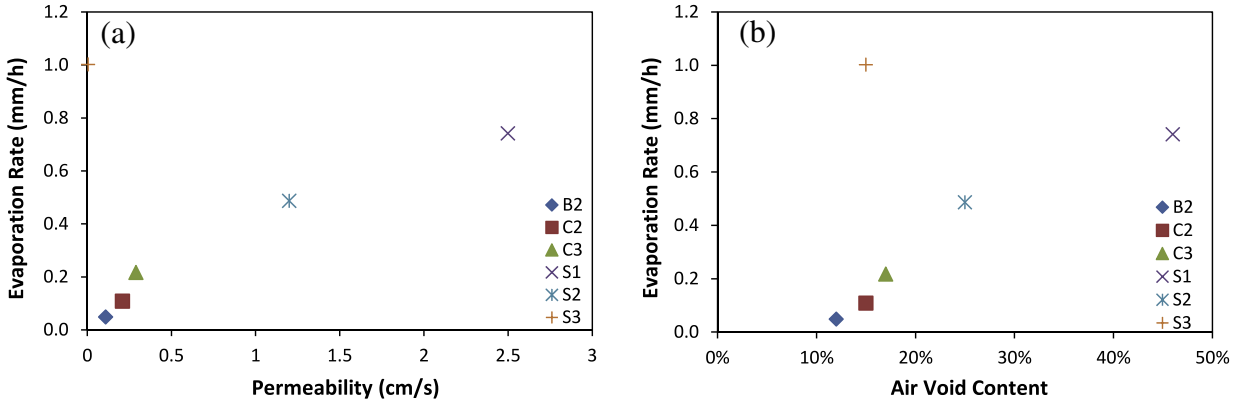

Fig. 10. Effects of permeability (a) and air void content (b) on evaporation rate.

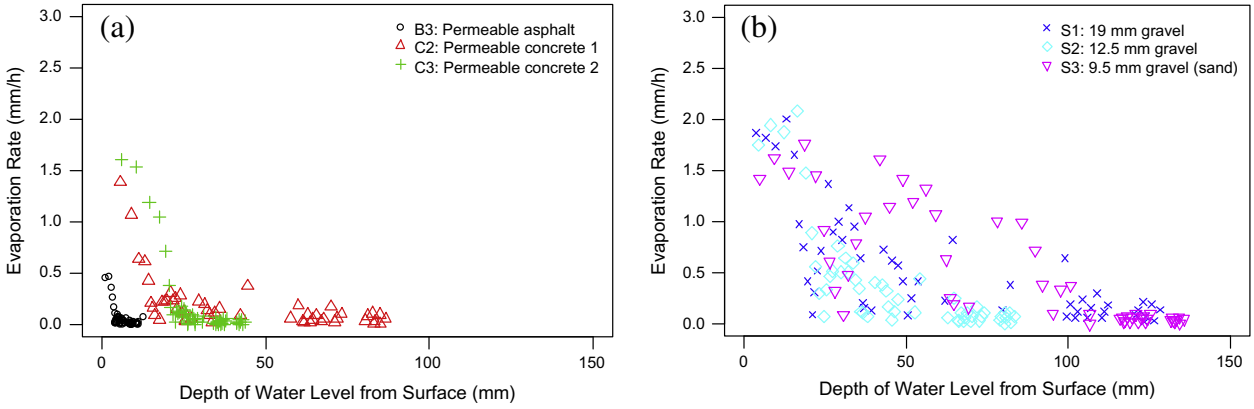

Fig. 11. Effects of water level depth on evaporation rate: (a) permeable surface materials and (b) gravel materials.

permeability tend to block the water evaporation from the materials and seal the moisture inside the materials.

As shown in Table 1, the fine but well graded sand S3 material (see Fig. 1 for the gradation) has the relatively smaller air void (15%) and low permeability (5×10^{-3} cm/s) among the six materials (S1, S2, S3, C3, C2 and B3). However, it has highest evaporation rate (1.0 mm/h, 3-day average) among all the six materials and its evaporation rate is just lower than but close to that of the bare water S0 (1.5 mm/h, 3-day average), as shown in Fig. 9(a) and (b)). The reason for this might be that, the fine sand material has small pore size, large surface area to volume ratio (SAVR) and consequently high capillary effect compared to the materials with large pore size (e.g. the permeable concrete C2 or gravel S1). The high capillary effect of the fine materials will easily move the water from the bottom of the material to the top or surface, enhancing the water availability near the surface of the materials and the consequent evaporation rate (see the discussion above). This suggests that improving the pore size and enhancing capillary effect of materials could help increase the evaporation rate. However, reducing the pore size and increasing the capillary effect might reduce the permeability. Therefore, an optimal design of material with optimized pore size and adequate permeability is desired.

All these findings imply again that high water availability near surface or moisture exposure to the atmosphere are critical for the

evaporation rate of pavement materials, as well as the high air temperature and low humidity. Increase in the air void and the permeability is one way to improve the water availability near surface or the moisture exposure to the atmosphere for the pavement materials. Keeping the surface wet through enhancing capillary effect or sprinkling water on surface is another way that could increase the evaporation rate and consequently produces a better evaporative cooling effect. The capillary effect depends on the air void content and structure in the surface materials and the size of air void (i.e. pore size). This needs more experimental and theoretical research to optimally design the materials, which is out of the scope of this paper and will be the next step of the study.

3.6. Effect of water level depth on evaporation rate

As the water evaporates the water level depth from the material surface increases. To explicitly examine the effect of water level depth on evaporation rate of permeable pavement materials, the relationships between evaporation rate and water level depth (estimated from remained water weight) are plotted in Fig. 11 for the three permeable surface materials (B3, C2 and C3, in (a)) and the three gravel materials (S1, S2 and S3, in (b)), respectively. It is clearly shown that the evaporation rate of permeable pavement materials decrease as the water level depth from the material surface increases. For the three permeable surface materials (Fig. 11(a)), the evaporation rate decreases significantly when the water level depth is over 20 mm. The evaporation rate decreases significantly when the water level depth is over 100 mm for the three gravel materials (Fig. 11(b)). This confirms again that the availability of water or moisture close to surfaces is very important for the evaporation rate.

4. Summary and conclusions

The evaporation rate is an important factor that influences the evaporative cooling effect of permeable pavements. It is determined by a complex system of factors, such as air temperature, relative humidity, water temperature, moisture content, air void content, content, air void size and connecting structure. To take an initial look at this complex system, a simple experiment method was used to measure the evaporation rates and explore the main factors affecting of different pavement materials under hot summer outdoor conditions at a test site in Davis, California. The results can provide some initial values of evaporation rate for the modeling and simulation of the cooling effect of evaporation from pavement. Some main findings from this experimental study include,

(a) The peak evaporation rate of bare water is about 2.0–2.5 mm/h during hot days with 3-day average of 1.5 mm/h, which is higher than that of water in any pavement materials tested.
(b) The 3-day average evaporation rate of gravel materials (S1, S2 and S3) is in the range of 0.5–1.0 mm/h. The fine sand with small pore size had a higher evaporation rate compared to the coarse gravel.
(c) The permeable asphalt and concrete pavement surface materials have 3-day average evaporation rates in the range of 0.1–0.3 mm/h, which is lower than the gravel materials due to their smaller air void content and lower permeability.
(d) Evaporation rate of pavement materials is high during the daytime, especially in the hot afternoon in summer, and low during the night time and especially in the cold early morning. High air temperature and low humidity will help enhance the evaporation rate, which is just what is expected under hot conditions.
(e) The air void and permeability are positively correlated to the evaporation rate for these permeable surface layer materials and permeable gravel materials except sand. A small air void and low permeability tend to block the water evaporation from the materials and seal the moisture inside the materials.
(f) Improving the pore size and enhancing capillary effect of materials could help increase the evaporation rate.

All these findings imply that high water availability near the surface or large moisture exposure to the atmosphere are critical for the evaporation rate of pavement materials, as well as the high air temperature and low humidity. Based on the findings, it can be concluded that increasing the air void and the permeability is one way to improve the moisture exposure to the atmosphere and enhance the evaporation for the pavement materials. Keeping the surface wet through enhancing capillary effect or sprinkling water on surface is another way that could increase the availability of water or moisture close to surfaces and the evaporation rate and consequently produces a better evaporative cooling effect. The capillary effect depends on the air void content and connecting structure in the surface materials and the size of air void (i.e. pore size). More experimental (e.g. with large sample size and sample number) and theoretical studies are recommended to evaluate and optimally design the evaporative cooling effect of pavement materials with adequate permeability.

Acknowledgements

The research was supported by a grant from the Sustainable Transportation Center at the University of California Davis, which receives funding from the U.S. Department of Transportation and Caltrans, the California Department of Transportation, through the University Transportation Centers program. The research activities described in this paper were also sponsored by the California Department of Transportation (Caltrans), Division of Research and Innovation. Both sponsorships are gratefully acknowledged. The contents of this paper reflect the views of the authors and do not reflect the official views or policies of the Sustainable Transportation Center or the State of California or the Federal Highway Administration.

References

[1] Kevern JT, Haselbach L, Schaefer VR. Hot weather comparative heat balances in pervious concrete and impervious concrete pavement systems. In: The second international conference on countermeasures to urban heat islands, Berkeley, California, US; 2009.
[2] Kevern JT, Schaefer VR, Wang KJ. Temperature behavior of pervious concrete systems. Transport Res Record 2009;2098:94–101.
[3] Stempihar J, Pourshams-Manzouri T, Kaloush K, Rodezno M. Porous asphalt pavement temperature effects for urban heat island analysis. Transport Res Record: J Transport Res Board 2012;2293(1):123–30.
[4] Golden JS, Kaloush KE. A hot night in the big city: how to mitigate the urban heat island. Public Works 2005;136(13).
[5] Kaloush KE, Carlson JD, Phelan PE. The Thermal and radiative characteristics of concrete pavements in mitigating urban heat island effects. Tempe, Arizona: National Center of Excellence on Sustainable Material and Renewable Technology (SMART) Innovations, Arizona State University; 2008. p. 139.
[6] Gui J, Phelan PE, Kaloush KE, Golden JS. Impact of pavement thermophysical properties on surface temperatures. J Mater Civil Eng 2007;19(8):683–90.
[7] Golden JS, Kaloush KE. Mesoscale and microscale evaluation of surface pavement impacts on the urban heat island effects. Int J Pavement Eng 2006;7(1):37–52.
[8] Carlson JD, Bhardwaj R, Phelan PE, Kaloush KE, Golden JS. Determining thermal conductivity of paving materials using cylindrical sample geometry. J Mater Civil Eng 2010;22(2):186–95.
[9] Belshe M, Kaloush KE, Golden JS, Mamlouk MS. The urban heat island effect and impact of asphalt rubber friction course overlays on Portland cement concrete pavements in the Phoenix area. 40971 ed. New Orleans, Louisiana: ASCE; 2008. p. 129.

[10] Golden JS, Carlson J, Kaloush KE, Phelan P. A comparative study of the thermal and radiative impacts of photovoltaic canopies on pavement surface temperatures. Solar Energy 2007;81(7):872–83.
[11] Xing Y, Handy SL, Mokhtarian PL. Factors associated with proportions and miles of bicycling for transportation and recreation in six small US cities. Transport Res D – Tr E 2010;15(2):73–81.
[12] Pucher J, Dill J, Handy S. Infrastructure, programs, and policies to increase bicycling: an international review. Prev Med 2010;50:S106–25.
[13] Saelens BE, Handy SL. Built environment correlates of walking: a review. Med Sci Sport Exer 2008;40(7):S550–66.
[14] Handy S, Cao XY, Mokhtarian PL. Self-selection in the relationship between the built environment and walking – empirical evidence from northern California. J Am Plann Assoc 2006;72(1):55–74.
[15] Handy SL, Boarnet MG, Ewing R, Killingsworth RE. How the built environment affects physical activity – views from urban planning. Am J Prev Med 2002;23(2):64–73.
[16] Hoehner CM, Ramirez LKB, Elliott MB, Handy SL, Brownson RC. Perceived and objective environmental measures and physical activity among urban adults. Am J Prev Med 2005;28(2):105–16.
[17] Handy SL, Cao XY, Mokhtarian PL. The causal influence of neighborhood design on physical activity within the neighborhood: evidence from Northern California. Am J Health Promot 2008;22(5):350–8.
[18] U.S. Green, Building Council. LEED for New Construction and Major Renovations Rating, System; 2009.
[19] Arnold CL, Gibbons CJ. Impervious surface coverage – the emergence of a key environmental indicator. J Am Plann Assoc 1996;62(2):243–58.
[20] Roseen R, DiGennaro N, Watts A, Ballestero T, Houle J. Preliminary results of the examination of thermal impacts from stormwater BMPs. World environmental and water resources congress; 2010. p. 3424–51.
[21] Roseen R, Ballestero T, Houle K, Heath D, Houle J. Assessment of winter maintenance of porous asphalt and its function for chloride source control. In: World environmental and water resources congress; 2013. p. 99–116.
[22] Roseen R, Ballestero T, Houle K, Briggs J, Houle J. Pervious concrete and porous asphalt pavements performance for stormwater management in northern climates. Cold regions engineering; 2009. p. 311–27.
[23] Roseen R, Ballestero T, Houle J, Briggs J, Houle K. Water quality and hydrologic performance of a porous asphalt pavement as a storm-water treatment strategy in a cold climate. J Environ Eng 2012;138(1):81–9.
[24] Houle K, Roseen R, Ballestero T, Briggs J, Houle J. Examinations of pervious concrete and porous asphalt pavements performance for stormwater management in northern climates. In: World environmental and water resources congress; 2009. p. 1–18.
[25] Li H, Harvey J, Jones D. Cooling effect of permeable asphalt pavement under both dry and wet conditions. Transport Res Record: J Transport Res Board 2013;3(2372):97–107.
[26] Li H, Harvey JT, Holland TJ, Kayhanian M. The use of reflective and permeable pavements as a potential practice for heat island mitigation and stormwater management. Environ Res Lett 2013;8(1):14.
[27] Li H, Harvey J, Kendall A. Field measurement of albedo for different land cover materials and effects on thermal performance. Build Environ 2013;59:536–46.
[28] Gartland L. Heat islands: understanding and mitigating heat in urban areas. London: Earthscan Press in UK and USA; 2008.
[29] Li H, Kayhanian M, Harvey J. Comparative field permeability measurement of permeable pavements using ASTM C1701 and NCAT permeameter methods. J Environ Manage 2013;118:144–52.
[30] Li H, Harvey J, Kendall A. Measurement of pavement solar reflectivity and effect on thermal performance. In: Transportation research board 92nd annual meeting. Washington, DC; 2013.